

## Mono-, Di-, and Tetrafluorinated Cyclams

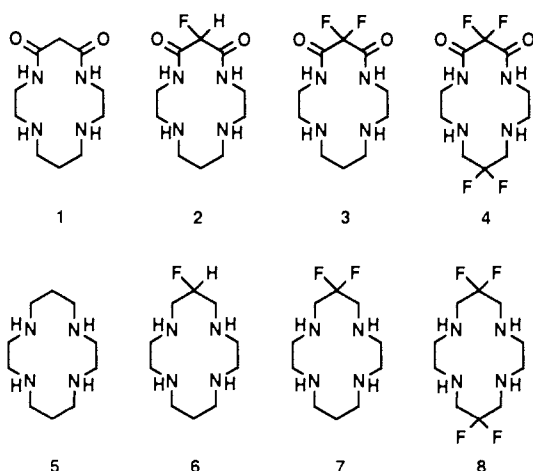
Mitsuhiko Shionoya,<sup>†</sup> Eiichi Kimura,<sup>\*,†,‡</sup> and Yoichi Iitaka<sup>§</sup>

Contribution from the Department of Medicinal Chemistry, School of Medicine, Hiroshima University, Kasumi, Minami-ku, Hiroshima 734, Japan, Coordination Chemistry Laboratories, Institute for Molecular Science, Myodaiji, Okazaki 444, Japan, and Physical Laboratory, Faculty of Pharmaceutical Science, Teikyo University, Kaga, Itabashi-ku, Tokyo 113, Japan.  
Received May 7, 1990

**Abstract:** A series of new mono-, di-, and tetrafluorinated dioxocyclams (2-4) and cyclams (6-8) has been synthesized and their complexing behaviors were investigated. The effects of the successive F substitutions were demonstrated by the drop in the amine basicities and the ligand field (LF) strengths in their Cu(II) and Ni(II) complexes. These are ascribable, though difficult to distinguish, to the strong electron-withdrawing effect and lipophilic effect characteristic of the F atom. Despite the weaker LF, the fluorinated dioxocyclams 2-4 generally form more stable Cu(II) complexes [Cu<sup>II</sup>(H<sub>2</sub>L)]<sup>0</sup> 19-21 than the nonfluorinated 1. In their kinetics in acetate buffers (4.7 < pH < 5.7), the fastest overall complexation was observed with the tetrafluorinated 4, where the contribution of the unprotonated ligand species is most determining. The Ni(II) complex with the tetrafluorinated cyclam 8 is in almost 100% high-spin state (blue, λ<sub>max</sub> 517 nm, ε 7) in 0.1 M NaClO<sub>4</sub> aqueous solution at 25 °C, while with nonfluorinated 5 it is in a mixture of high- and low-spin states. The X-ray crystal structure of the Ni<sup>II</sup>-8·Cl<sub>2</sub> has been resolved by the heavy-atom method using 1550 unique reflections with I > 2σ(I). Final R was 0.056: monoclinic space group P2<sub>1</sub>/n with a = 14.218 (8) Å, b = 8.524 (5) Å, c = 6.538 (5) Å, β = 98.46 (5)°, and V = 783.7 Å<sup>3</sup>; d<sub>calcd</sub> = 1.703 g cm<sup>-3</sup> for Z = 2, and mol wt 401.9. The purple 8 complex has a 6-coordinate octahedral structure with square-planar nitrogens and two axial chlorides. The bonding parameters are not appreciably different from those of the 5 complex. From the cyclic voltammetry of the series of Cu<sup>II</sup>(H<sub>2</sub>L) (18-21) and Ni<sup>II</sup>L (22-25) in aqueous solution, as the number of F increases, both the oxidation processes for Cu<sup>II</sup> = Cu<sup>III</sup> and Ni<sup>II</sup> = Ni<sup>III</sup> and the reduction process for Ni<sup>II</sup> = Ni<sup>I</sup> show anodic shifts compared to the nonfluorinated analogues. To explore useful applications, the Ni(II)-fluorinated cyclam complexes 23-25 were tested as electroreduction catalysts for CO<sub>2</sub> → CO in H<sub>2</sub>O. The efficiency of (CO + H<sub>2</sub>) products yield and the CO/H<sub>2</sub> selectivity depend upon the number of fluorine atoms. The tetrafluorinated complex 25 works more efficiently and selectively at a lower energy of -1.10 V vs SCE than the nonfluorinated cyclam complex 22 does.

## Introduction

Cyclam (1,4,8,11-tetraazacyclotetradecane, 5) has long been an extremely useful and versatile tetraamine ligand in coordination chemistry, bioinorganic and biomimetic chemistry, or catalysis.<sup>1</sup> Recently, new cyclam structures have been synthesized by incorporation of carbonyl group(s) adjacent to the amines of monooxocyclam (5-oxo-1,4,8,11-tetraazacyclotetradecane)<sup>2a</sup> and dioxocyclam (5,7-dioxo-1,4,8,11-tetraazacyclotetradecane, 1)<sup>2</sup> or by attachment of pendant donors such as phenol,<sup>3,4</sup> catechol,<sup>5</sup> pyridine,<sup>6,7</sup> and imidazole<sup>8</sup> to the cyclam carbon skeleton. These new cyclam derivatives have brought new dimensions to the conventional cyclam chemistry.<sup>9</sup>



We now have turned to another way to functionalize the cyclam without changing the basic structure. Historically, fluorine substitution of hydrogens in organic molecules has been a promising method in searching for renewed functions, while retaining essentially the same stereochemical features. Recent success in

synthesis of fluorinated malonates under mild conditions<sup>10</sup> has led us to conceive a design to replace the skeletal C-H for C-F in the cyclam propylene chains. Then, it would be of interest to

- (1) (a) Hinz, F. P.; Margerum, D. W. *J. Am. Chem. Soc.* **1974**, *96*, 4993. (b) Beley, M.; Collin, J.-P.; Ruppert, R.; Sauvage, J.-P. *J. Am. Chem. Soc.* **1986**, *108*, 7461, and references cited therein. (c) Grant, J. L.; Goswami, K.; Spreer, L. O.; Otvos, J. W.; Calvin, M. *J. Chem. Soc., Dalton Trans.* **1987**, 2105. (d) Kimura, E.; Wada, S.; Shionoya, M.; Takahashi, T.; Iitaka, Y. *J. Chem. Soc., Chem. Commun.* **1990**, 397. (e) Tsukube, H. *J. Chem. Soc., Perkin Trans. 1* **1985**, 615. (f) Taniguchi, I.; Nakashima, N.; Yasukouchi, K. *J. Chem. Soc., Chem. Commun.* **1986**, 1814. (g) Loncin, M. F.; Desreux, J. F.; Merciny, E. *Inorg. Chem.* **1986**, *25*, 2646. (h) Kunitake, T.; Ishikawa, Y.; Shimomura, M. *J. Am. Chem. Soc.* **1986**, *108*, 327. (i) Ram, M. S.; Espenson, J. M.; Bakac, A. *Inorg. Chem.* **1986**, *25*, 4115. (j) Blake, A. J.; Gould, R. O.; Hyde, T. I.; Schröder, M. *J. Chem. Soc., Chem. Commun.* **1987**, 431. (k) Bond, A. M.; Khalita, M. A. *Inorg. Chem.* **1987**, *26*, 413. (l) Kooraa, J. D.; Kochi, J. K. *Inorg. Chem.* **1987**, *26*, 908. (m) Takiguchi, T.; Nonaka, T. *Chem. Lett.* **1987**, 1217. (n) Wagler, T. R.; Fang, Y.; Burrows, J. C. *J. Org. Chem.* **1989**, *54*, 1584. (o) Yoon, H.; Burrows, J. C. *J. Am. Chem. Soc.* **1988**, *110*, 4087.
- (2) (a) Kimura, E.; Koike, T.; Machida, R.; Nagai, R.; Kodama, M. *Inorg. Chem.* **1984**, *23*, 4181. (b) Kimura, E. *J. Coord. Chem.* **1986**, *15*, 1. (c) Ishizu, I.; Hirai, J.; Kodama, M.; Kimura, E. *Chem. Lett.* **1979**, 1045. (d) Hay, R. W.; Pujari, M. P.; McLaren, F. *Inorg. Chem.* **1984**, *23*, 3033. (e) Kimura, E.; Sakonaka, A.; Machida, R. *J. Am. Chem. Soc.* **1982**, *104*, 4255. (f) Kimura, E.; Dalimunte, C. A.; Yamashita, A.; Machida, R. *J. Chem. Soc., Chem. Commun.* **1985**, 1041. (g) Fabbri, L.; Kaden, T. A.; Perotti, A.; Seghi, B.; Siegfried, L. *Inorg. Chem.* **1986**, *25*, 321. (h) Kimura, E.; Lin, Y.; Machida, R.; Zenda, H. *J. Chem. Soc., Chem. Commun.* **1986**, 1020. (i) Kobayashi, N.; Zao, X.; Osa, T.; Kato, K.; Hanabusa, K.; Imoto, T.; Shirai, H. *J. Chem. Soc., Dalton Trans.* **1987**, 1801.
- (3) Kimura, E.; Koike, T.; Takahashi, M. *J. Chem. Soc., Chem. Commun.* **1985**, 385.
- (4) Kimura, E.; Koike, T.; Uenishi, K.; Hediger, M.; Kuramoto, M.; Joko, S.; Arai, Y.; Kodama, M.; Iitaka, Y. *Inorg. Chem.* **1987**, *26*, 2975.
- (5) Kimura, E.; Joko, S.; Koike, T.; Kodama, M. *J. Am. Chem. Soc.* **1987**, *109*, 5528.
- (6) Kimura, E.; Koike, T.; Nada, H.; Iitaka, Y. *J. Chem. Soc., Chem. Commun.* **1986**, 1322.
- (7) Kimura, E.; Koike, T.; Nada, H.; Iitaka, Y. *Inorg. Chem.* **1988**, *27*, 1036.
- (8) Kimura, E.; Shionoya, M.; Mita, T.; Iitaka, Y. *J. Chem. Soc., Chem. Commun.* **1987**, 1712.
- (9) Kimura, E. *Pure Appl. Chem.* **1989**, *61*, 823.
- (10) Umemoto, T.; Kawada, K.; Tomita, K. *Tetrahedron Lett.* **1986**, 4465. **9b** was synthesized from diethyl 2-fluoromalonnate by using the fluorinating reagent, *N*-fluoro-2,4,6-trimethylpyridinium triflate, developed by Umemoto and co-workers.

<sup>†</sup>Hiroshima University.<sup>‡</sup>Institute for Molecular Science.<sup>§</sup>Teikyo University.

see the changes in properties of the fluorinated cyclams and their metal complexes.

Of particular interest with the fluorinations are the effect on (i) basicities of the amines, (ii) the rate of cyclam complexation, (iii) stability of metal complexes, (iv) oxidation states of the encapsulated metal ions, (v) low-spin and high-spin equilibrium with Ni(II)-cyclam complexes, and (vi) ligand lipophilicity and on the resulting complex behaviors. Study on these subjects would at the same time help further clarify the characteristics of cyclam complexations, which have been extensively studied and yet sometimes subjected to debate.<sup>1,2</sup>

Earlier, we synthesized mono- and difluorinated dioxocyclams (2 and 3) and cyclams (6 and 7) and their interesting properties were communicated.<sup>11</sup> We now have completed the synthesis of tetrafluorinated dioxocyclam 4 and cyclam 8, and in this article we present a full account of the whole ligand series of cyclams.

### Experimental Section

**General Methods.** All the starting materials for synthesis were obtained commercially and were used without further purification. Aqueous solutions were prepared from analytical grade salts and redistilled water. Gases of analytical grade were used without further purification. Melting points were determined by using a Yanako micro melting point apparatus and were uncorrected. <sup>1</sup>H NMR spectra were obtained on a Hitachi R-40 high-resolution NMR spectrometer (90 MHz, 35 °C, Me<sub>4</sub>Si reference) or a JEOL GX-400 spectrometer (400 MHz, 35 °C, Me<sub>4</sub>Si reference). IR and mass spectra were obtained on Shimadzu FTIR-4200 and JEOL JMS-01SG-2 spectrometers, respectively. UV-visible spectra were recorded on a Hitachi U-3200 double-beam spectrophotometer or a Shimadzu UV-3100 spectrophotometer at 25.0 ± 0.1 °C, using matched quartz cells of 2-, 10-, or 50-mm path length. ESR spectra at 77 K were recorded on a JES-FE1X spectrometer using Mn<sup>II</sup>-doped MgO powder as reference ( $g_3 = 2.034$  and  $g_4 = 1.981$ ). For TLC analysis throughout this work, Merck precoated TLC plates (silica gel 60 F<sub>254</sub>) were used. Column chromatography was carried out on silica gel (Wakogel C-300).

**Potentiometric Titrations.** Aqueous solutions (50 mL) of ligands (1.00 × 10<sup>-3</sup> M) with 2 equiv of HClO<sub>4</sub> (2.00 × 10<sup>-3</sup> M) for 1-4 or with 4 equiv of HClO<sub>4</sub> (4.00 × 10<sup>-3</sup> M) for 5-8 and 13 in the absence (for determination of ligand protonation constants log  $K_a$ ) or presence of equivalent metal ion (for determination of complexation constants) were titrated with carbonate-free 0.100 M NaOH aqueous solution. pH values were read with an Orion 811 digital pH meter. The temperature was maintained at 25.00 ± 0.05 °C, and ionic strength was adjusted to 0.10 M with NaClO<sub>4</sub>. -log [H<sup>+</sup>] values were estimated with a correction of -0.08 pH unit to the pH meter readings.<sup>12</sup> All the solutions were carefully protected from air by a stream of humidified Ar. The electrode system was calibrated with pH 4.01 and 7.00 standard buffer solutions and checked by the duplicate theoretical titration curves of 4.00 × 10<sup>-3</sup> M HClO<sub>4</sub> with a 0.100 M NaOH solution at 25 °C and  $I = 0.10$  M (NaClO<sub>4</sub>) in low- and high-pH regions.

**Electrochemical Measurements.** Cyclic voltammetry was performed with a Yanako P-1100 polarographic analyzer at 25.00 ± 0.05 °C. A three-electrode system was employed: a 3-mm glassy carbon rod (Tokai Electrode Co. GC-30) or hanging mercury electrode as the working electrode, a Pt wire as the counter electrode, and a saturated calomel electrode (SCE) as the reference electrode. The cyclic voltammograms with scan rates of 100-200 mV/s were evaluated graphically.

Controlled-potential electrolysis experiments were performed in a gas-tight electrolysis cell with a Yanako VE-8 controlled-potential electrolyzer. The gas-tight cell was a 50-mL three-necked, round-bottomed flask equipped with three side arms. Mercury was used as the working electrode (14 mL; purity >99.9%). The counter electrode (Pt) and the reference electrode (SCE) were separated from the working electrode compartment. The cell volume was 142 mL, of which 108 mL was occupied by gases. The aqueous solution (20 mL) was degassed before electrolysis by bubbling CO<sub>2</sub> through it for 30 min. The internal pressure within the electrolysis cell was kept equal to 1 atm by using syringe techniques. Turnover frequencies were calculated as moles of CO produced per mole of an electrocatalyst in 1 h.

**Analytical Methods for CO<sub>2</sub> Reduction.** Gas samples (0.5 mL), taken at various intervals with a gas-tight syringe through a septum and a valve, were analyzed for H<sub>2</sub> on a Shimadzu GC-8A gas chromatograph

**Table I.** Crystal Data of Ni(II) Complex 25·Cl<sub>2</sub>

formula	C <sub>10</sub> H <sub>20</sub> N <sub>4</sub> F <sub>4</sub> Cl <sub>2</sub> Ni
$M_r$	401.9
cryst syst	monoclinic
space group	$P2_1/n$
cryst color	purple
cell dimens	
$a$ , Å	14.218 (8)
$b$ , Å	8.524 (5)
$c$ , Å	6.538 (5)
$\beta$ , deg	98.46 (5)
$V$ , Å <sup>3</sup>	783.7
$Z$	2
$d_{\text{calcd}}$ , g cm <sup>-3</sup>	1.703
cryst dimens, mm	0.05 × 0.1 × 0.2 Cu K $\alpha$
radiation	Cu K $\alpha$ (graphite monochromated)
$\mu$ , cm <sup>-1</sup>	54.0
$2\theta$ range, deg	6-156
scan speed, deg min <sup>-1</sup>	6
phasing	heavy-atom method
no. of measd reflns	1572
no. of indep reflns ( $I > 2\sigma(I)$ )	1550
final $R$	0.056

**Table II.** Final Fractional Coordinates (×10<sup>4</sup> for Non-Hydrogen Atoms and ×10<sup>3</sup> for Hydrogen Atoms) for 25·Cl<sub>2</sub><sup>a</sup>

atom	$x$	$y$	$z$	$B_{\text{eq}}$ , Å <sup>2</sup>
Ni	0 (0)	0 (0)	0 (0)	1.95 (0.01)
N(1)	-1436 (2)	517 (5)	-146 (6)	3.7 (0.1)
C(2)	-1749 (3)	-345 (6)	1617 (7)	2.8 (0.1)
C(3)	-1303 (3)	-1953 (6)	1755 (7)	2.7 (0.1)
N(4)	-246 (2)	-1752 (5)	2037 (5)	3.4 (0.1)
C(5)	242 (4)	-3252 (6)	1847 (8)	3.0 (0.1)
C(6)	1302 (4)	-3027 (6)	1927 (8)	3.2 (0.1)
C(7)	1700 (3)	-2182 (6)	231 (8)	3.1 (0.1)
F(6)	1654 (2)	-2329 (4)	3799 (5)	4.3 (0.1)
F(6)	1693 (2)	-4513 (4)	2029 (6)	5.3 (0.1)
Cl(1)	443 (1)	1775 (1)	2991 (2)	2.9 (0.0)
HN(1)	-182 (5)	3 (8)	-161 (10)	6.7 (1.8)
HC(2)	-153 (4)	28 (7)	298 (9)	4.4 (1.4)
H'C(2)	-249 (4)	-44 (7)	141 (9)	4.8 (1.4)
HC(3)	-154 (4)	-260 (7)	37 (9)	4.9 (1.4)
H'C(3)	-152 (4)	-258 (7)	302 (8)	4.1 (1.3)
HN(4)	1 (4)	-133 (8)	363 (9)	5.4 (1.5)
HC(5)	-2 (5)	-378 (7)	41 (9)	4.2 (1.3)
H'C(5)	14 (4)	-402 (7)	308 (9)	4.5 (1.4)
HC(7)	143 (4)	-273 (7)	-123 (9)	5.1 (1.5)
H'C(7)	245 (4)	-231 (7)	47 (8)	4.0 (1.3)

<sup>a</sup> Estimated standard deviation in parentheses.

equipped with a thermal conductivity detector by using a 3 m × 2.6 mm o.d. column packed with molecular sieves 13X-S at 50 °C using N<sub>2</sub> as carrier gas, or a Shimadzu GC-4CMPF FID gas chromatograph, and for CO with a Shimadzu MTN-1 methanizer using N<sub>2</sub> as carrier gas.

**Kinetic Measurements.** The rates of [Cu<sup>II</sup>(H<sub>2</sub>L)]<sup>0</sup> complex formation with dioxocyclams 1-4 at 25 °C and  $I = 0.1$  (NaClO<sub>4</sub>) were measured with an Otsuka Electronics Photol RA-401 stopped-flow spectrophotometer system. Concentrations were [L] = [Cu<sup>II</sup>] = 1.0 mM and acetate buffers (50 mM) were used to cover the pH region (4.7 < pH < 5.7). The ionic strength was kept constant at 0.1 M with NaClO<sub>4</sub>. The reactions were monitored at 505 (1), 518 (2), 515 (3), and 526 nm (4) by measuring the increase in absorbance due to the formation of [Cu<sup>II</sup>(H<sub>2</sub>L)]<sup>0</sup>. The observed rate constants were analyzed as previously reported.<sup>13,14</sup>

**Crystallographic Study.** A purple prism of the Ni(II) complex 25·Cl<sub>2</sub> with dimensions 0.05 × 0.1 × 0.2 mm<sup>3</sup> was used for data collection at room temperature. The lattice parameters and intensity data were measured on a Philips PW-1100 automatic four-circle diffractometer by using graphite-monochromated Cu K $\alpha$  radiation. Crystal data and data collection parameters are displayed in Table I. The structure was solved by the heavy-atom method refined by the block-diagonal-matrix least-squares method to  $R$  value of 0.056. The molecular structure is illustrated in Figure 3 by ORTEP drawings with 50% probability thermal ellipsoids. The atomic positional parameters are given together with their

(11) Kimura, E.; Shionoya, M.; Okamoto, M.; Nada, H. *J. Am. Chem. Soc.* **1988**, *110*, 3679.

(12) *Kagaku Binran*, 3rd ed.; Chemical Society of Japan: Tokyo, 1984; Vol. 11.

(13) Kodama, M.; Kimura, E. *J. Chem. Soc., Dalton Trans.* **1977**, 1473.

(14) Kodama, M.; Kimura, E. *J. Chem. Soc., Dalton Trans.* **1979**, 327.

Table III. Bond Distances (Å) for 25·Cl<sub>2</sub><sup>a</sup>

N(1)–C(2)	1.489 (6)	C(6)–F(6)	1.387 (6)
N(1)–C(7)	1.467 (7)	C(6)–F'(6)	1.381 (6)
C(2)–C(3)	1.507 (7)	C(7)–N(1)	1.467 (7)
C(3)–N(4)	1.498 (6)	Ni–N(1)	2.077 (4)
N(4)–C(5)	1.470 (6)	Ni–N(4)	2.064 (4)
C(5)–C(6)	1.512 (7)	Ni–Cl(1)	2.479 (1)
C(6)–C(7)	1.501 (8)		

<sup>a</sup> Estimated standard deviations in parentheses.Table IV. Bond Angles (Degrees) for 25·Cl<sub>2</sub><sup>a</sup>

C(2)–N(1)–C(7)	113.8 (4)	C(5)–C(6)–F(6)	106.1 (4)
C(3)–C(2)–N(1)	108.9 (4)	F(6)–C(6)–F'(6)	105.1 (4)
N(4)–C(3)–C(2)	108.0 (4)	N(1)–C(7)–C(6)	111.7 (4)
C(5)–N(4)–C(3)	111.5 (4)	N(1)–Ni–N(4)	85.69 (15)
C(6)–C(5)–N(4)	111.5 (4)	N(1)–Ni–Cl	92.34 (11)
C(7)–C(6)–C(5)	121.2 (4)	N(1)–Ni–N'(4)	94.31 (15)
C(7)–C(6)–F(6)	108.6 (4)	N(1)–Ni–Cl	87.66 (11)
C(7)–C(6)–F'(6)	106.4 (4)	N(4)–Ni–Cl	88.86 (10)
C(5)–C(6)–F(6)	108.3 (4)		

<sup>a</sup> Estimated standard deviations in parentheses.

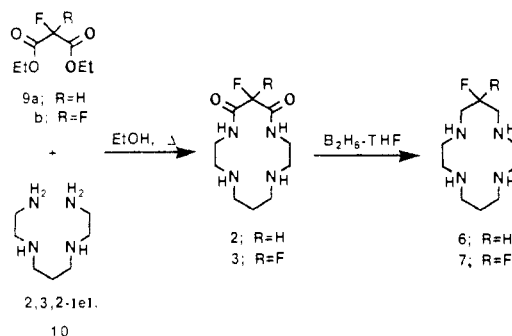
standard deviations in Table II. Selected bond distances and angles are presented in Tables III and IV, respectively. A listing of thermal parameters for the Ni(II) complex 25·Cl<sub>2</sub> and tables of observed and calculated structure factors for the complex are in the supplementary material.

**Synthesis (Schemes I and II).** 6-Fluoro-5,7-dioxo-1,4,8,11-tetraazacyclotetradecane (2) and 6-fluoro-1,4,8,11-tetraazacyclotetradecane (6). Refluxing 9a<sup>15</sup> (3.00 g, 16.8 mmol) and 1,9-diamino-3,7-diazanonane (10, 2,3,2-tet; 2.70 g, 16.8 mmol) in 360 mL of EtOH for 3 h afforded 6-fluoro-5,7-dioxo-1,4,8,11-tetraazacyclotetradecane (2) as colorless needles (1.72 g), after purification by silica gel column chromatography (eluent, CH<sub>2</sub>Cl<sub>2</sub>–CH<sub>3</sub>OH–28% aqueous NH<sub>3</sub>, 50:5:1) and recrystallization from CH<sub>3</sub>CN. Reduction of the monofluorinated dioxocyclam 2 (492 mg, 2.0 mmol) with diborane (B<sub>2</sub>H<sub>6</sub>) in tetrahydrofuran (THF) (1.0 M, Aldrich) and subsequent treatment with aqueous HCl yielded monofluorinated cyclam 6 as its tetrahydrochloride salt, which was passed through a column of strong base anion-exchange resin (Amberlite IRA-400) with water to get the free form of 6. The residue after evaporation was purified by recrystallization from CH<sub>3</sub>CN to give colorless needles (311 mg). The melting point, analytical results (C, N, H), and some of physical properties of 2–4 and 6–8 are summarized in Table V.

**6,6-Difluoro-5,7-dioxo-1,4,8,11-tetraazacyclotetradecane (3) and 6,6-Difluoro-1,4,8,11-tetraazacyclotetradecane (7).** Refluxing 9b<sup>10</sup> (1.15 g, 5.9 mmol) and 2,3,2-tetraamine 10 (0.94 g, 5.9 mmol) in 140 mL of EtOH for 3 h afforded 6,6-difluoro-5,7-dioxo-1,4,8,11-tetraazacyclotetradecane (3) as colorless needles (556 mg), after purification by silica gel column chromatography (eluent, CH<sub>2</sub>Cl<sub>2</sub>–CH<sub>3</sub>OH–28% aqueous NH<sub>3</sub>, 50:5:1) and recrystallization from CH<sub>3</sub>CN. Reduction of the difluorinated dioxocyclam 3 (264 mg, 1.0 mmol) with B<sub>2</sub>H<sub>6</sub>–THF yielded difluorinated cyclam 7 (143 mg) after a similar workup and purification as for 2.

**6,6,13,13-Tetrafluoro-5,7-dioxo-1,4,8,11-tetraazacyclotetradecane (4) and Its Monohydrochloride Salt (4·HCl).** Refluxing of 9b (4.7 g, 24 mmol) and mono-N-triphenylmethylated ethylenediamine 11 (14.6 g, 48 mmol) in 250 mL of EtOH for 3 h under Ar afforded 12 as a precipitate. The product was recrystallized from acetone to give 12 as colorless prisms (11.3 g, 66%): mp 200.0–200.5 °C; IR (Nujol) ν<sub>C=O</sub> 1692 cm<sup>-1</sup>; <sup>1</sup>H NMR (400 MHz, CDCl<sub>3</sub>) δ 1.5–1.8 (br, 2 H, amide NH), 2.34 (t, J = 4 Hz, 4 H), 3.39 (t, J = 4 Hz, 4 H), 7.1–7.3 (m, 18 H), 7.3–7.5 (m, 12 H). Reduction of the amide 12 (7.1 g, 10 mmol) with B<sub>2</sub>H<sub>6</sub>–THF yielded difluoro-2,3,2-tetraamine tetrahydrochloride 13·4HCl (1,9-diamino-3,7-diaza-5,5-difluorononane tetrahydrochloride; 2.82 g, 82%) after removal of the protecting group by HCl: mp 218–226 °C dec; <sup>1</sup>H NMR (400 MHz, D<sub>2</sub>O) δ 3.38–3.47 (m, 4 H), 3.47–3.56 (m, 4 H), 3.81 (t, J = 16 Hz, 4 H). 13·4HCl (1.0 g, 2.9 mmol) was quickly passed through a column of Amberlite IRA-400 (50 mL in wet volume) with water to yield the monohydrochloride (13·HCl) as a major product and a small proportion of the free form of 13. This mixture and diethyl difluoromalonate (9b; 600 mg, 3.1 mmol) in 60 mL of EtOH were stirred under Ar at room temperature for 46 h. The reaction mixture was concentrated and the resulting residue was recrystallized from CH<sub>3</sub>CN–MeOH (2:1) to give 209 mg of colorless prisms as the monohydrochloride salt (4·HCl).

Scheme I



The mother liquid after the recrystallization was evaporated and chromatographed on silica gel (gradient elution with CH<sub>2</sub>Cl<sub>2</sub>–CH<sub>3</sub>OH, 50–30:1) to obtain the free form of tetrafluorinated dioxocyclam 4 as colorless needles (32 mg), *m/z* 300 (M<sup>+</sup>).

**6,6,13,13-Tetrafluoro-1,4,8,11-tetraazacyclotetradecane (8).** Reduction of 4·HCl (337 mg, 1.0 mmol) with B<sub>2</sub>H<sub>6</sub>–THF yielded tetrafluorinated cyclam 8 as a colorless solid after the usual workup. The product was purified by recrystallization from isopropyl alcohol to obtain colorless needles (200 mg).

**Preparation of the Copper(II) Complexes with Dioxocyclams 1–4.** A ligand (0.5 mmol) and CuSO<sub>4</sub>·5H<sub>2</sub>O (125 mg, 0.5 mmol) were dissolved in 50 mL of 0.5 M Na<sub>2</sub>SO<sub>4</sub> aqueous solution at ca. 25 °C, and the mixture was adjusted to pH 8 with 0.1 M NaOH aqueous solution. The resulting solution was filtered, and the filtrate was allowed to stand several weeks at room temperature to precipitate crystalline [Cu<sup>II</sup>(H<sub>2</sub>L)]<sup>0</sup> 19–21 (L = 2–4). The nonfluorinated complex 18 (L = 1) was prepared as previously described.<sup>16</sup> Anal. Calcd (Found) for 19 (blue prisms) C<sub>10</sub>H<sub>17</sub>O<sub>2</sub>N<sub>4</sub>FCu·0.5H<sub>2</sub>O: C, 36.86 (36.63); H, 5.88 (5.77); N, 17.20 (17.13). Anal. Calcd (Found) for 20 (blue prisms) C<sub>10</sub>H<sub>16</sub>O<sub>2</sub>N<sub>4</sub>F<sub>2</sub>Cu·1.5H<sub>2</sub>O: C, 34.04 (34.25); H, 5.43 (5.16); N, 15.88 (15.99). Anal. Calcd (Found) for 21 (dark red prisms) C<sub>10</sub>H<sub>14</sub>O<sub>4</sub>N<sub>4</sub>F<sub>4</sub>Cu·H<sub>2</sub>O: C, 31.62 (31.88); H, 4.25 (4.23); N, 14.75 (14.58).

**Preparation of Ni(II) Complexes with Cyclams 6–8. Method A.** A ligand (0.5 mmol) and NiSO<sub>4</sub> (77 mg, 0.5 mmol) were dissolved in 50 mL of 0.1 M NaClO<sub>4</sub> aqueous solution at 50 °C, and the mixture was adjusted to pH 7 with 0.1 M NaOH solution. The solutions were allowed to stand for several weeks at room temperature to obtain complexes. Anal. Calcd (Found) for [Ni<sup>II</sup>–6](ClO<sub>4</sub>)<sub>2</sub>·H<sub>2</sub>O [or 23·(ClO<sub>4</sub>)<sub>2</sub>·H<sub>2</sub>O] (orange prisms) C<sub>10</sub>H<sub>23</sub>O<sub>8</sub>N<sub>4</sub>FCu·H<sub>2</sub>O: C, 24.32 (24.34); H, 5.10 (4.87); N, 11.34 (11.52). Anal. Calcd (Found) for [Ni<sup>II</sup>–7](ClO<sub>4</sub>)<sub>2</sub>·2H<sub>2</sub>O [or 24·(ClO<sub>4</sub>)<sub>2</sub>·2H<sub>2</sub>O] (orange prisms) C<sub>10</sub>H<sub>22</sub>O<sub>8</sub>N<sub>4</sub>F<sub>2</sub>Cl<sub>2</sub>Ni·2H<sub>2</sub>O: C, 22.66 (22.95); H, 4.95 (4.68); N, 10.57 (10.80). [Ni<sup>II</sup>–8](ClO<sub>4</sub>)<sub>2</sub>·*n*H<sub>2</sub>O [or 25·(ClO<sub>4</sub>)<sub>2</sub>·*n*H<sub>2</sub>O] (yellow prisms, recrystallized from EtOH) was very hygroscopic and immediately changed to violet in air. The nonfluorinated cyclam complex [Ni<sup>II</sup>–5](ClO<sub>4</sub>)<sub>2</sub> [or 22·(ClO<sub>4</sub>)<sub>2</sub>] was prepared according to the literature.<sup>17</sup>

**Method B.** The complexes as the dichloride, 23·Cl<sub>2</sub>–25·Cl<sub>2</sub>, were prepared by the same method as for 22·Cl<sub>2</sub>.<sup>17</sup> A single crystal of 25·Cl<sub>2</sub> suitable for X-ray crystallographic study was obtained by recrystallization from water. Anal. Calcd (Found) for [Ni<sup>II</sup>–6]Cl<sub>2</sub> (or 23·Cl<sub>2</sub>) C<sub>10</sub>H<sub>23</sub>N<sub>4</sub>FCuCl<sub>2</sub>Ni: C, 34.52 (34.04); H, 6.66 (6.53); N, 16.10 (15.94). Anal. Calcd (Found) for [Ni<sup>II</sup>–7]Cl<sub>2</sub> (or 24·Cl<sub>2</sub>) C<sub>10</sub>H<sub>22</sub>N<sub>4</sub>F<sub>2</sub>Cl<sub>2</sub>Ni·0.5EtOH: C, 33.97 (33.65); H, 6.48 (6.41); N, 14.40 (14.52). Anal. Calcd for [Ni<sup>II</sup>–8]Cl<sub>2</sub> (or 25·Cl<sub>2</sub>) C<sub>10</sub>H<sub>20</sub>N<sub>4</sub>F<sub>4</sub>Cl<sub>2</sub>Ni: C, 29.89 (29.77); H, 5.02 (5.09); N, 13.94 (14.07).

## Results and Discussion

**Synthesis of the Fluorinated Cyclam Ligands.** The synthesis of the mono- (2) and difluorine-containing (3) dioxocyclams was easily achieved by condensation of each corresponding fluorine-substituted malonic ester (9a and 9b, respectively) with 1,9-diamino-3,7-diazanonane (10) in refluxing EtOH (see Scheme I). The corresponding cyclams 6 and 7 were obtained by reduction of 2 and 3 with B<sub>2</sub>H<sub>6</sub>–THF. These procedures are analogous to the one employed for nonfluorinated cyclam.<sup>18</sup> However, the cyclization process goes much faster with more fluorines (e.g., for 3, within 3 h, yield 36%; while for 1, 72 h, yield ~30%). The

(16) Kodama, M.; Kimura, E. *J. Chem. Soc., Dalton Trans.* **1981**, 694.  
 (17) Bosnich, B.; Tobe, M. L.; Webb, G. A. *Inorg. Chem.* **1965**, *4*, 1109.  
 (18) Tashiro, I.; Taniguchi, Y.; Kato, H. *Tetrahedron Lett.* **1977**, 1049.

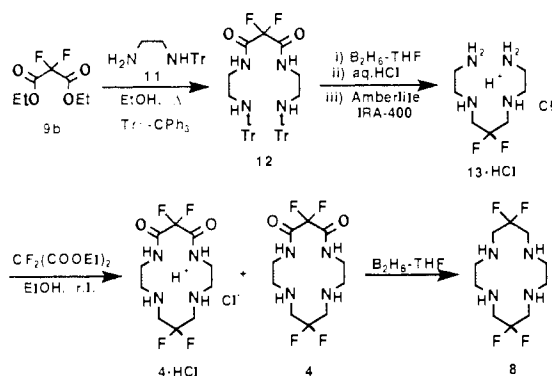
(15) Bergmann, E. D.; Cohen, S.; Shakak, I. *J. Chem. Soc.* **1959**, 3286.

Table V. Various Properties of New Ligands

ligands	mp, °C	yield, %	Anal. (C,H,N) <sup>c</sup>	IR (Nujol) <sup>d</sup> $\nu_{C=O}$ , cm <sup>-1</sup>	<sup>1</sup> H NMR, $\delta$
2	194.0–194.5	39 <sup>a</sup>	C <sub>10</sub> H <sub>19</sub> O <sub>2</sub> N <sub>4</sub> F	1688	(CDCl <sub>3</sub> ) 1.5–1.9 (m, 2 H), 1.90 (br, 2 H), 2.4–3.0 (m, 4 H), 3.2–3.8 (m, 4 H), 5.23 (d, <i>J</i> 48 Hz, 1 H), 7.45 (br, 2 H)
3	179.5–180.0	36 <sup>a</sup>	C <sub>10</sub> H <sub>18</sub> O <sub>2</sub> N <sub>4</sub> F <sub>2</sub> ·0.5H <sub>2</sub> O	1705	(CDCl <sub>3</sub> ) 1.4–1.8 (m, 2 H), 1.77 (d, <i>J</i> 24 Hz, 3 H), 2.4–3.0 (m, 10 H), 3.0–3.4 (m, 2 H), 3.4–3.8 (m, 2 H), 7.35 (br, 2 H)
4·HCl	220–250 (dec)	20 <sup>a</sup>	C <sub>10</sub> H <sub>17</sub> O <sub>2</sub> N <sub>4</sub> F <sub>4</sub> Cl	1736 (s), 1694 (w)	(D <sub>2</sub> O) 2.93 (t, <i>J</i> 5 Hz, 4 H), 3.24 (t, <i>J</i> 13 Hz, 4 H), 3.41 (t, <i>J</i> 5 Hz, 4 H)
4 (free)	214.0–214.5	4 <sup>a</sup>	C <sub>10</sub> H <sub>16</sub> O <sub>2</sub> N <sub>4</sub> F <sub>4</sub>	1705	(CD <sub>3</sub> OD) 2.81 (t, <i>J</i> 5 Hz, 4 H), 2.96 (t, <i>J</i> 13 Hz, 4 H) 3.43 (t, <i>J</i> 5 Hz, 4 H)
6	170.0–172.0	71 <sup>b</sup>	C <sub>10</sub> H <sub>23</sub> N <sub>4</sub> F		(CDCl <sub>3</sub> ) 1.5–1.9 (m, 2 H), 2.1 (br, 4 H), 2.6–2.9 (m, 12 H), 2.9–3.2 (m, 4 H), 4.70 (dm, <i>J</i> 45 Hz, 1 H)
7	148.5–149.0	61 <sup>b</sup>	C <sub>10</sub> H <sub>22</sub> N <sub>4</sub> F <sub>2</sub>		(D <sub>2</sub> O) 1.5–1.6 (m, 2 H), 2.5–2.7 (m, 12 H), 2.87 (t, <i>J</i> 13 Hz, 4 H)
8	106.5–107.0	73 <sup>b</sup>	C <sub>10</sub> H <sub>20</sub> N <sub>4</sub> F <sub>4</sub>		(D <sub>2</sub> O as 4HCl salts) 2.96 (s, 8 H), 3.36 (t, <i>J</i> 12 Hz, 8 H)

<sup>a</sup>Cyclization yield. <sup>b</sup>Reduction yield. <sup>c</sup>Compounds gave satisfactory analyses ( $\pm 0.4\%$ ). <sup>d</sup>Compare with 1662 cm<sup>-1</sup> for 1.

Scheme II



introduction of fluorine(s) activates the malonate ester, as indicated by the increasing  $\nu_{C=O}$  frequency (Nujol): 1730 cm<sup>-1</sup> (ethyl malonate), 1745 and 1770 cm<sup>-1</sup> (monofluorinated **9a**), and 1780 cm<sup>-1</sup> (difluorinated **9b**).

The synthesis of tetrafluorinated cyclams was not as easy as initially planned and the method outlined in Scheme II was the most appropriate one. The treatment of ethyl difluoromalonate (**9b**) with mono-*N*-triphenylmethylated ethylenediamine **11** in refluxing EtOH gave the amide **12**. Reduction of the amide **12** with B<sub>2</sub>H<sub>6</sub>-THF and the subsequent partial neutralization with a strong base anion-exchange resin (Amberlite IRA-400) yielded a key intermediate, difluorinated 2,3,2-tetraamine **13** as the monohydrochloride. This linear tetraamine monohydrochloride was then treated with equivalent **9b** in EtOH at room temperature to obtain the desired cyclic product, tetrafluorinated dioxocyclam **4** (isolated as a monohydrochloride salt in 20% yield and as a free form in 4% yield). If this cyclization is run with free **13**, the degradation of **13** occurs, resulting in a poorer yield of **4**. Finally, the reduction of the diamide group of **4** was carried out with B<sub>2</sub>H<sub>6</sub>-THF to the symmetric, tetrafluorinated cyclam **8** (see Table V). As predicted, the unprotonated tetrafluorinated dioxocyclam **4** and cyclam **8** are most lipophilic, while the nonfluorinated dioxocyclam **1** and cyclam **5** are most hydrophilic. Similar trends are also seen in their metal complexes.

**Basicities of the Fluorinated Cyclams.** With a series of fluorinated dioxocyclams and cyclams in hand, systematic investigation of the amine basicities, which is the simplest diagnosis of the fluorination effect, has become possible. The deprotonation constants ( $pK_n$ ) of macrocyclic dioxocyclams **1–4** and cyclams **5–8**, and linear tetraamines **10** and **13** determined by potentiometric titrations at 25 °C and *I* = 0.1 M (NaClO<sub>4</sub>) (Figures 1 and 2) are summarized in Table VI.

A far-reaching basicity-weakening effect by the fluorine atom(s), although it is weak, is apparent by comparing  $pK_1$  and  $pK_2$  values for the two remote secondary nitrogens among dioxocyclams **1–3**. This may not reflect a direct electron-withdrawing effect but rather an indirect one through weakened hydrogen bondings between the less electron donating amide oxygens and the protons attached to the N lone pairs. An additional pair

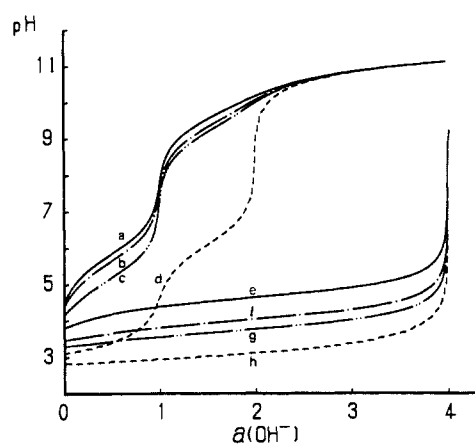


Figure 1. pH titration curves of diprotonated dioxocyclams **1–4** with NaOH in the absence and the presence of equimolar Cu(II) at 25 °C and *I* = 0.1 M (NaClO<sub>4</sub>). Key: (a) 1.00 mM **1**·2H<sup>+</sup>; (b) 1.00 mM **2**·2H<sup>+</sup>; (c) 1.00 mM **3**·2H<sup>+</sup>; (d) 1.00 mM **4**·2H<sup>+</sup>; (e) a + 1.00 mM Cu<sup>II</sup>SO<sub>4</sub>; (f) b + 1.00 mM Cu<sup>II</sup>SO<sub>4</sub>; (g) c + 1.00 mM Cu<sup>II</sup>SO<sub>4</sub>; (h) d + 1.00 mM Cu<sup>II</sup>SO<sub>4</sub>.

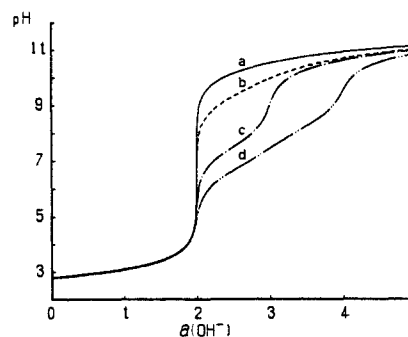


Figure 2. pH titration curves of tetraprotonated cyclams H<sub>4</sub>L<sup>4+</sup> **5–8** with NaOH at 25 °C and *I* = 0.1 M (NaClO<sub>4</sub>). Key: (a) 1.00 mM **5**·4H<sup>+</sup>; (b) 1.00 mM **6**·4H<sup>+</sup>; (c) 1.00 mM **7**·4H<sup>+</sup>; (d) 1.00 mM **8**·4H<sup>+</sup>.

Table VI. Deprotonation Constants of Polyamines at 25 °C and *I* = 0.1 (NaClO<sub>4</sub>)

	$pK_1$	$pK_2$	$pK_3$	$pK_4$
<b>1</b> ·2H <sup>+</sup>	9.63	5.85		
<b>2</b> ·2H <sup>+</sup>	9.37	5.65		
<b>3</b> ·2H <sup>+</sup>	9.22	5.18		
<b>4</b> ·2H <sup>+</sup>	6.10	~1.9		
<b>5</b> ·4H <sup>+</sup>	11.78	10.55	~1.7 <sup>a</sup>	~1.0 <sup>a</sup>
<b>6</b> ·4H <sup>+</sup>	10.96	9.41	<2	<1
<b>7</b> ·4H <sup>+</sup>	10.78	7.52	<2	<1
<b>8</b> ·4H <sup>+</sup>	8.22	6.70	<2	<1
<b>10</b> ·4H <sup>+</sup> <sup>b</sup>	9.99	9.29	7.46	5.49
<b>13</b> ·4H <sup>+</sup>	9.86	9.11	4.58	2.42

<sup>a</sup> Kodama, M.; Kimura, E. *J. Chem. Soc., Dalton Trans.* **1976**, 1721.  
<sup>b</sup> From ref 17.

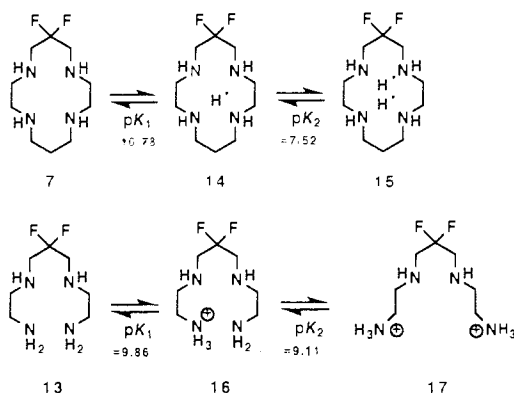
**Table VII.** IR, Visible Absorption, Stability Constants, ESR Parameters of Cu(II)-Deprotonated Dioxocyclam Complexes [Cu<sup>II</sup>(H<sub>2</sub>L)]<sup>0</sup> **18–21**, and Their Half-Wave Potentials (V vs SCE) for Cu(III/II)

Complexes	IR <sub>C=O</sub> <sup>a</sup> cm <sup>-1</sup>	visible λ <sub>max</sub> , nm (ε) <sup>b</sup>	log K(CuH <sub>2</sub> L) <sup>c</sup>	ESR(77 K) <sup>d</sup>			E <sub>1/2</sub> Cu(III/II) <sup>e</sup>	
				g <sub>⊥</sub>	g <sub>∥</sub>	A <sub>∥</sub> , G	in H <sub>2</sub> O <sup>f</sup>	in DMF <sup>g</sup>
<b>18</b> (L = <b>1</b> )	1580	505 (100)	0.11 ± 0.01	2.06	2.17	215	+0.64	<i>h</i>
<b>19</b> (L = <b>2</b> )	1575	518 (137)	0.49 ± 0.03	2.06	2.18	217	+0.69	<i>h</i>
<b>20</b> (L = <b>3</b> )	1620	515 (108)	2.5 ± 0.2	2.06	2.18	217	+0.83	<i>h</i>
<b>21</b> (L = <b>4</b> )	1652	526 (95)	0.84 ± 0.01	2.06	2.18	212	<i>i</i>	+0.85

<sup>a</sup>Nujol. <sup>b</sup>At 25 °C, 0.5 M Na<sub>2</sub>SO<sub>4</sub>; ε, M<sup>-1</sup> cm<sup>-1</sup>. <sup>c</sup>K(CuH<sub>2</sub>L) defined by [CuH<sub>2</sub>L][H<sup>+</sup>]<sup>2</sup>/[Cu<sup>II</sup>][L] M (at 25 °C, 0.1 M NaClO<sub>4</sub>). <sup>d</sup>0.5 M Na<sub>2</sub>SO<sub>4</sub>. <sup>e</sup>All solutions were deaerated by purified Ar and a Pt wire was used as auxiliary electrode. <sup>f</sup>0.5 M (Na<sub>2</sub>SO<sub>4</sub>), 25 °C, pH 7.0. Working electrode (WE), glassy carbon. <sup>g</sup>0.1 M NaClO<sub>4</sub> in DMF, 25 °C, WE; glassy carbon. <sup>h</sup>**18–20** were insoluble in DMF. <sup>i</sup>The oxidation process did not occur in water.

of the fluorine atoms (to **4**) exerts a direct and hence dramatic effect on these amine basicities (pK<sub>1</sub> = 6.10 and pK<sub>2</sub> ~ 1.9).

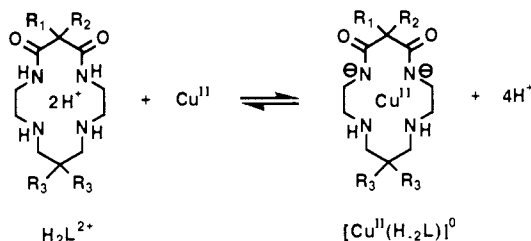
A similar basicity-weakening effect is exemplified by the difluorinated cyclam **7** (to **14**, pK<sub>1</sub> = 10.78), as compared with that



(pK<sub>1</sub> = 11.78) of the nonfluorinated **5**. The second proton would go to a nitrogen closer to the fluorine atoms (to **15**), which comes under stronger influence of the fluorine(s), pK<sub>2</sub> = 7.52, much lower than 10.55 for **5**. Such a large drop in the basicity of the monoprotonated cyclam **14** is in good contrast to the small drop in the corresponding linear tetraamine homologue (pK<sub>2</sub> = 9.29 for **10**,<sup>19</sup> and pK<sub>2</sub> = 9.11 for **13**), which is accounted for by the different site of the second protonation. The introduction of difluorines to both sides of the propylene (i.e., **8**) dramatically lowers pK<sub>1</sub> and pK<sub>2</sub> values to 8.22 and 6.70, respectively.

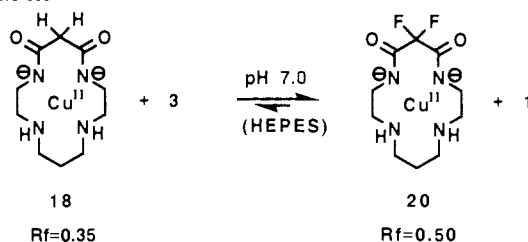
In addition to the electron-pulling effect, the lipophilic nature of F may also be responsible for the lower pK<sub>a</sub> values by preventing water molecules from accessing the protonated nitrogen atoms so as to destabilize the protonated cyclams.

**Copper(II) Complexes with Dioxocyclams 1–4.** The pH titration curves for all of the fluorinated dioxocyclams **2–4** (as H<sub>2</sub>L<sup>2+</sup>) in the presence of equivalent Cu(II) ion under Ar at 25 °C (Figure 1) are similar to the one for **1** with occurrence of the first inflections at *a* = 4,<sup>13,16</sup> indicating the simultaneous dissociation of the two protons (from the secondary amine) and the two amide hydrogens to form complexes having a common formula [Cu<sup>II</sup>(H<sub>2</sub>L)]<sup>0</sup> **18–21**. However, each titration time became longer



- 1: R<sub>1</sub>=R<sub>2</sub>=R<sub>3</sub>=H  
 2: R<sub>1</sub>=F, R<sub>2</sub>=R<sub>3</sub>=H  
 3: R<sub>1</sub>=R<sub>2</sub>=F, R<sub>3</sub>=H  
 4: R<sub>1</sub>=R<sub>2</sub>=R<sub>3</sub>=F

- 18: R<sub>1</sub>=R<sub>2</sub>=R<sub>3</sub>=H  
 19: R<sub>1</sub>=F, R<sub>2</sub>=R<sub>3</sub>=H  
 20: R<sub>1</sub>=R<sub>2</sub>=F, R<sub>3</sub>=H  
 21: R<sub>1</sub>=R<sub>2</sub>=R<sub>3</sub>=F

**Scheme III**

as more F was incorporated, with **4** being the slowest (more than 60 min at the equilibrium pH < 4; see Figure 1). This is due to the fact that the copper(II) is least accessible to the least basic secondary amines of the tetrafluorinated **4**. (However, at pH > 4.5, the complexation of **4** is fastest; see the kinetics section below.) The complexation constants K(CuH<sub>2</sub>L) ([CuH<sub>2</sub>L][H<sup>+</sup>]<sup>2</sup>/[Cu<sup>II</sup>][L] M)<sup>13,16</sup> calculated from Figure 1 are summarized in Table VII.

It is interesting that the stability constants of the fluorinated complexes **19–21** are generally greater than that of the parent nonfluorinated **18**. The stability peaks at the difluorinated complex **20**. This stability order is supported by the qualitative observation. Using different R<sub>f</sub> values on silica gel TLC (eluent, CH<sub>3</sub>OH), one can easily follow the ligand substitution reactions. For instance, one sees **18** disappear as **20** appears, but does not see the reverse reaction (Scheme III). On the basis of the d–d absorption maxima of **18–21** in aqueous solution (see Table VII), the sequence of the square-planar LF strength of Cu<sup>II</sup>(H<sub>2</sub>L) is **18** (non-F) > **20** (di-F) ~ **19** (mono-F) > **21** (tetra-F). However, with the more lipophilic **20**, the free energy loss by the ligand desolvation (prior to complexation) may not be as big as with the hydrophilic **18**. Overall, the most favorable free energy change would occur to **20**.

All of the [Cu<sup>II</sup>(H<sub>2</sub>L)]<sup>0</sup> complexes **18–21** were isolable as crystalline products, whose physical properties are listed in Table VII. The strong electron-withdrawing of F atom(s) from the two proximate imide nitrogens is well reflected in the higher stretching frequencies of the amide carbonyl ν<sub>C=O</sub> as more fluorines are incorporated. The ESR parameters for the paramagnetic [Cu<sup>II</sup>(H<sub>2</sub>L)]<sup>0</sup> complexes are almost similar among the series, indicating a similar, rigid macrocyclic square-planar N<sub>4</sub> ligand field.

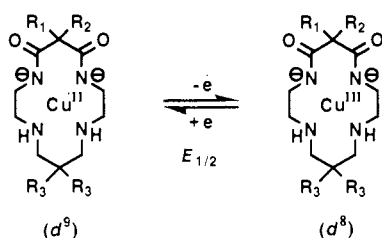
We had earlier found that the uncommon Cu(III), Ni(III) oxidation states are kinetically and thermodynamically stabilized by deprotonated macrocyclic oxopolyamine ligands.<sup>2b</sup> A new family of macrocyclic polyamine ligands containing amide functions has been developed.<sup>9</sup> The cavity size, number of amide functions, type of appended substituents, and the number and type of donor atoms affect their redox properties.<sup>9</sup> The present mono- and difluorodioxocyclam complexes Cu(H<sub>2</sub>L) **19** and **20** showed quasi-reversible cyclic voltammograms for Cu(III/II) in a fashion similar to the nonfluorinated Cu(H<sub>2</sub>L) **18** in 0.5 M Na<sub>2</sub>SO<sub>4</sub> aqueous solution at 25 °C (Table VII). This oxidation process, however, did not occur to the tetrafluoro **21** in water. The Cu(III) in the most lipophilic **21** may not be sufficiently stabilized by waters. However, in dimethylformamide (DMF), a quasi-reversible cyclic voltammogram was seen for **21** at E<sub>1/2</sub> = +0.85 vs SCE (0.1 M NaClO<sub>4</sub>, 25 °C). The less fluorinated Cu(II)

**Table VIII.** Formation Rate Constants of  $[\text{Cu}^{\text{II}}(\text{H}_{-2}\text{L})^0]$  (Where L = 1–4) in Acetate Buffers at 25 °C and  $I = 0.1 \text{ M}$  ( $\text{NaClO}_4$ )<sup>a</sup>

ligands [L]	$10^{-2}k_{\text{obs}}$ ( $\text{M}^{-1} \text{s}^{-1}$ )			resolved rate const. <sup>b</sup> $\text{M}^{-1} \text{s}^{-1}$		ligand forms at pH 5.2, <sup>d</sup> %		contribution of $k_L$ term at pH 5.2, %
	pH 5.60	pH 5.20	pH 4.80	$k_L$	$k_{\text{HL}}$	[L]	[HL] <sup>+</sup>	
1	11.0	4.68	2.85	~0	$(3.1 \pm 0.4) \times 10^3$ <sup>c</sup>	$5.9 \times 10^{-4}$	16	~0
2	9.76	3.32	1.36	$(8.0 \pm 1.0) \times 10^6$	$(8.5 \pm 1.0) \times 10^2$	$1.6 \times 10^{-3}$	24	39
3	12.5	4.41	1.35	$(6.1 \pm 0.2) \times 10^6$	$(2.4 \pm 0.2) \times 10^2$	$4.8 \times 10^{-3}$	50	71
4	71.0	31.8	13.5	$(2.9 \pm 0.1) \times 10^4$	~0	12	88	~100

<sup>a</sup> Initial concentrations:  $[\text{L}] = [\text{Cu}^{\text{II}}] = 1.0 \text{ mM}$ ,  $[\text{MeCO}_2^-] = 50 \text{ mM}$ . <sup>b</sup>  $k_{\text{obs}}(\alpha_{\text{H}})_L = k_L + k_{\text{HL}}[\text{H}^+]/K_1$  [where  $(\alpha_{\text{H}})_L = 1 + [\text{H}^+]/K_1 + [\text{H}^+]^2/K_1K_2$ ]. <sup>c</sup> The same value with the literature data<sup>14</sup> for 1:  $k_{\text{HL}} = (3.1 \pm 0.3) \times 10^3 \text{ M}^{-1} \text{ s}^{-1}$ ,  $[\text{L}] = [\text{Cu}^{\text{II}}] = 5.0 \text{ mM}$ , and  $[\text{MeCO}_2^-] = 0.1 \text{ M}$  at 25 °C and  $I = 0.2 \text{ M}$ . <sup>d</sup> Calculated by using Table VI.

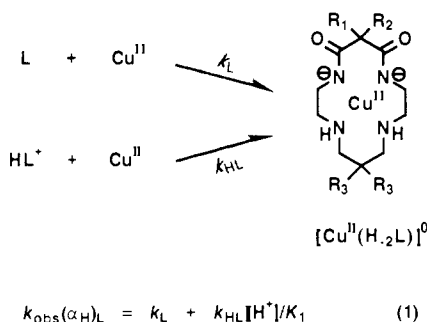
complexes (18–20) were insoluble in DMF. Naturally, the fluorination weakens the  $\sigma$ -donor abilities of the imide anions and hence the higher oxidation state Cu(III) successively becomes destabilized with respect to Cu(II).



#### Kinetics of the Cu(II) Complexation with Dioxocyclams 1–4.

The rates have been measured for  $[\text{Cu}^{\text{II}}(\text{H}_{-2}\text{L})^0]$ , L = 2–4, formation in acetate buffers ( $4.7 < \text{pH} < 5.7$ ) at 25 °C and  $I = 0.1 \text{ M}$  ( $\text{NaClO}_4$ ) to compare with the previously reported kinetics for L = 1.<sup>14</sup> At any given pH, the observed second-order rate constant  $k_{\text{obs}}$  was greatest with the tetrafluorinated 4 (see Table VIII). This was ascribed to the fact that the tetrafluorinated 4 exists appreciably in the unprotonated form (see Table VIII).

At a constant concentration of acetate, all  $k_{\text{obs}}$  for 2–4 could be resolved by eq 1 as for L = 1,<sup>14</sup> where  $(\alpha_{\text{H}})_L = 1 + [\text{H}^+]/K_1$

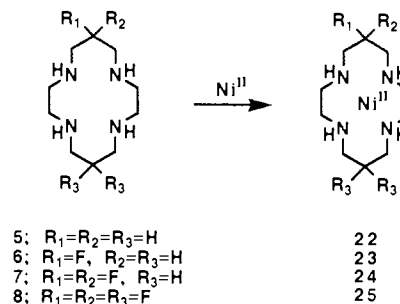


+  $[\text{H}^+]^2/K_1K_2$ , and  $k_L$  and  $k_{\text{HL}}$  are the rate constants for unprotonated and monoprotonated forms of the ligands, respectively. The rate constants  $k_L$  (from intercepts) and  $k_{\text{HL}}$  (from slope) were determined by linear plots of  $k_{\text{obs}}(\alpha_{\text{H}})_L$  vs  $[\text{H}^+]$  and the results are summarized in Table VIII. To check, we also have measured  $k_{\text{obs}}$  for L = 1.

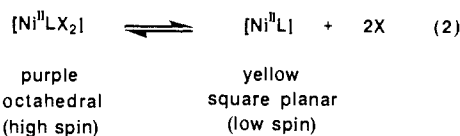
As the number of fluorine atoms increases, the resolved rate constants  $k_L$  and  $k_{\text{HL}}$  decrease, accompanied by the increase in the contribution of the  $k_L$  term to the overall reaction. With tetrafluorinated dioxocyclam 4, the rate constant  $k_{\text{HL}}$  for the monoprotonated species is negligible despite its greater abundance of 88% vs 12% of the unprotonated form at pH 5.2 (see Table VIII). Accordingly, only the  $k_L$  term  $[(2.9 \pm 0.1) \times 10^4]$  contributes to the overall rate of the Cu(II) complexation. On the other hand, with nonfluorinated 1, the  $k_{\text{HL}}$  term exclusively determines  $k_{\text{obs}}$ . Among  $k_L$  for L = 2–4 or  $k_{\text{HL}}$  for L = 1–3, the values become smaller as the number of F increases. These results are readily understood by considering the weakening donor ability of the nitrogen atoms.

**Ni(II) Complexes with Fluorinated Cyclams 5–8.** We were unable to conduct potentiometric titrations for the Ni(II) complexation constants with cyclams 6–8 (like 5), due to extremely

slow kinetics<sup>20</sup> and also to instability of some of the fluorinated ligands.



However, treatment of Ni(II) with cyclams, L = 5–8, in neutral pH solution yielded stable 1:1  $[\text{Ni}^{\text{II}}\text{L}]^{2+}$  complexes 22–25. It is well documented that tetraaza macrocyclic complexes of Ni(II) are in equilibrium between blue (high-spin, octahedral) and yellow (low-spin, square-planar) species (eq 2), and that the ligand electronic and steric features affect this equilibrium.<sup>21</sup>



The fluorination effect on the complex structure is assessed by measurement of the Ni(II) spin states, which is monitored spectrophotometrically by use of the low-spin-specific absorption bands ( $\lambda_{\text{max}}$  445, 451, 459, and 476 nm for 22–25, respectively). For 22–24, the equilibrium 2 shifts to the right by increasing temperature and the ionic strength, converging to a leveling yellow diamagnetic form at 35 °C and  $I = 5 \text{ M}$   $\text{NaClO}_4$ . We thus estimated the limiting  $\epsilon$  values at 45 and 36 for 100% low-spin complexes 23 and 24, respectively.

With the nonfluorinated cyclam complex 22, the low-spin Ni(II) (71%) dominates over the high-spin Ni(II) (29%) in 0.1 M  $\text{NaClO}_4$  aqueous solution at 25 °C.<sup>21a</sup> The proportion of the high-spin state increases as the number of fluorine atoms increases (see Table IX) and the tetrafluorinated cyclam complex 25 remains in a blue, high-spin form in 0.1 M  $\text{NaClO}_4$  aqueous solution at <30 °C. It is conceivable that the in-plane cyclam ligand field becomes weaker by the increasing fluorines with the lowering antibonding  $d_{x^2-y^2}$  energy level to stabilize the high-spin state of Ni(II). The energy of the single visible band  $\nu(\text{d-d})$  for yellow low-spin  $\text{Ni}^{\text{II}}$  complexes reflects the  $D_q^{sp}$  value and represents the strength of Ni–N in-plane interactions.<sup>21b</sup> Indeed,  $\nu(\text{d-d})$  decreases with more fluorine substitution (Table IX).

**Crystal Structure of Ni(II) Complex with Tetrafluorinated Cyclam 8 as a Dichloride.** The X-ray study (Figure 3) has proved

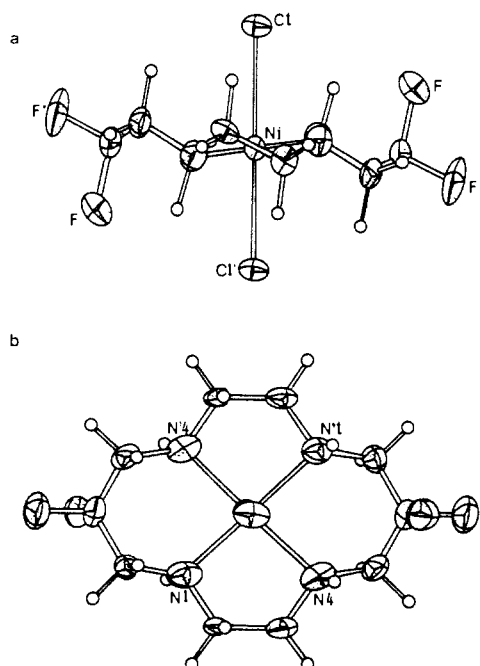
(20) Hinz, F. P.; Margerum, D. W. *Inorg. Chem.* **1974**, *13*, 2941.

(21) For dioxo tetraamines: References 2a,b and 16. For dioxo-free tetraamines: (a) Anichini, A.; Fabbri, L.; Paoletti, P. *Inorg. Chim. Acta*, **1977**, *24*, L21. (b) Fabbri, L. *Inorg. Chem.* **1977**, *16*, 2667. (c) Fabbri, L. *J. Chem. Soc., Dalton Trans.* **1979**, 1857. (d) Sabatini, L.; Fabbri, L. *Inorg. Chem.* **1979**, *18*, 438. (e) Fabbri, L.; Micheloni, M.; Paoletti, P. *Inorg. Chem.* **1980**, *19*, 535.

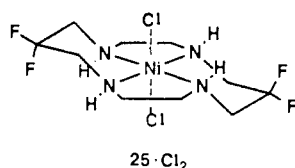
**Table IX.** Visible Absorption Maxima and Metal Spin States of Ni(II) Complexes **22**·(ClO<sub>4</sub>)<sub>2</sub>–**25**·(ClO<sub>4</sub>)<sub>2</sub>, Energy of the d–d Absorption Band ( $\nu_{d-d}$ ) for 100% Low-Spin Complexes, and Half-Wave Potentials (V vs SCE)<sup>e</sup> for Ni(III/II) and Ni(II/I).

Ni(II) complexes [Ni <sup>II</sup> L]	$\lambda_{max}$ , nm ( $\epsilon$ , M <sup>-1</sup> cm <sup>-1</sup> )	Ni(II) spin state, <sup>a</sup> %		$\nu_{d-d}$ , <sup>c</sup> cm <sup>-1</sup>	$E_{1/2}$ (V vs SCE)	
		high-spin form	low-spin form		Ni(III/II) <sup>f</sup>	Ni(II/I) <sup>g</sup>
<b>22</b> ·(ClO <sub>4</sub> ) <sub>2</sub> (L = <b>5</b> ) <sup>b</sup>	445 (46)	29	71	22 740	+0.50	-1.56
<b>23</b> ·(ClO <sub>4</sub> ) <sub>2</sub> (L = <b>6</b> )	451 (28)	38	62	22 030	+0.52	-1.52
<b>24</b> ·(ClO <sub>4</sub> ) <sub>2</sub> (L = <b>7</b> )	504 (6)	86	14	21 650	+0.63	-1.46
<b>25</b> ·(ClO <sub>4</sub> ) <sub>2</sub> (L = <b>8</b> )	517 (7)	>99	<1	~21 000 <sup>d</sup>	+0.81	-1.42

<sup>a</sup> At equilibrium in 0.1 M NaClO<sub>4</sub> aqueous solution at 25 °C. <sup>b</sup> See ref 19b. <sup>c</sup> Energy values of the d–d absorption band for 100% low-spin complexes were determined in >5 M NaClO<sub>4</sub> aqueous solution. <sup>d</sup> The limiting  $\epsilon$  value for low-spin species of **25** could not be determined accurately because precipitation occurred before reaching its limit. <sup>e</sup> All solutions were deaerated by purified Ar and a Pt wire was used as auxiliary electrode. <sup>f</sup> 0.5 M (Na<sub>2</sub>SO<sub>4</sub>), 25 °C, pH 6–7. WE: glassy carbon. <sup>g</sup> 0.1 M (NaClO<sub>4</sub>), 25 °C, pH 7.0. WE: hanging mercury drop electrode.

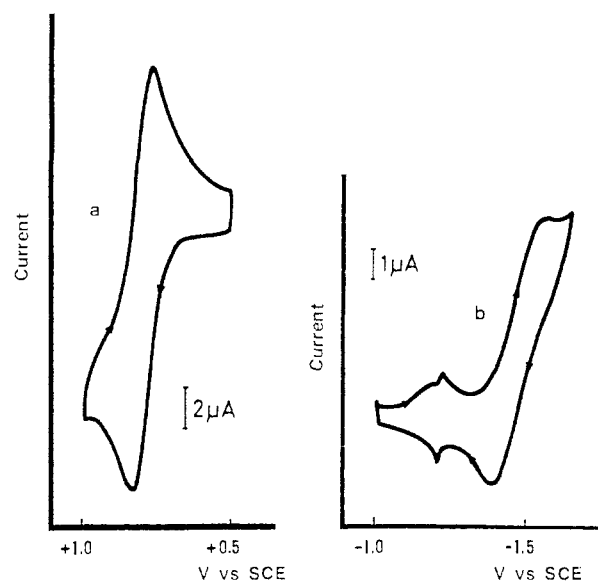
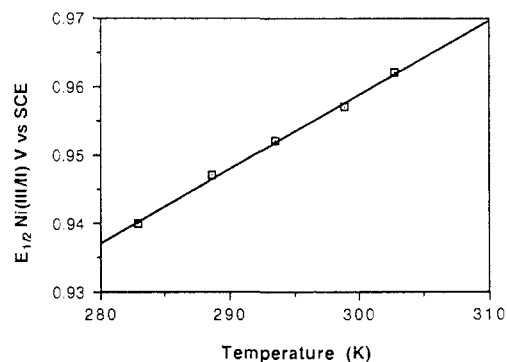
**Figure 3.** ORTEP drawing of **25**·Cl<sub>2</sub>. (a) Side-on view, (b) top view. Atoms are drawn with 50% probability thermal ellipsoids.

that the **25**·Cl<sub>2</sub> complex has a high-spin octahedral structure with four square-planar nitrogens and two axial chlorides.



The *R,R,S,S*- (or *trans*-III)<sup>22</sup> configuration of the macrocyclic ligand **8** is identical with that of the high-spin nonfluorinated cyclam complex **22**·Cl<sub>2</sub>.<sup>23</sup> The nickel ion is coplanar with N<sub>4</sub>. Interestingly, the four equatorial Ni–N bond distances, 2.077 (4) Å (Ni–N1, Ni–N8) and 2.064 (4) Å (Ni–N4, Ni–N11) Å, are not so elongated from those for the nonfluorinated cyclam **5** complex **22**·Cl<sub>2</sub> [2.067 (1) and 2.066 (1) Å, respectively].<sup>23b</sup> Accordingly, the average axial Ni–Cl bond length [2.479 (1) Å] is not so appreciably shorter than that for **22**·Cl<sub>2</sub> [2.5101 (4) Å].<sup>23b</sup> From these results, one might suspect that the square-planar nonfluorinated cyclam configuration is fully expanded and the F substitutions cannot affect it any more.

**Redox Properties of Ni(II)–Cyclam Complexes **22**–**25**.** In the cyclam complex **22**, Ni(II) can be reversibly reduced to Ni(I) ( $E_{1/2}$

**Figure 4.** Cyclic voltammograms of the Ni<sup>II</sup>-**8** complex [**25**·(ClO<sub>4</sub>)<sub>2</sub>]. (a) Ni(III/II) redox couple in 0.5 M Na<sub>2</sub>SO<sub>4</sub> at 25 °C, using a glassy carbon electrode at 200 mV/s. (b) Ni(II/I) redox couple in 0.1 M NaClO<sub>4</sub> at 25 °C, using a hanging mercury electrode at 200 mV/s.**Figure 5.** Dependence of the Ni(III/II) redox change in the high-spin Ni(II) complex with **8** upon temperature at 0.1 M NaClO<sub>4</sub> and pH 2.2, using a glassy carbon as a working electrode.

= -1.56 V vs SCE) and oxidized to Ni(III) ( $E_{1/2}$  = +0.50 V vs SCE) in aqueous solutions (Table IX). The present fluorination was expected to destabilize the Ni(III) state and to stabilize the Ni(I) state. The cyclic voltammograms of the fluorinated cyclam complexes **22**–**25** (in 0.5 M Na<sub>2</sub>SO<sub>4</sub> aqueous solution at 25 °C)<sup>24</sup> showed all reversible Ni(III/II) redox behaviors, with the peak potential separation of 70 mV (scan rate, 100 mV/s) and the peak current ratios of unity (for **25**, see Figure 4a). The redox potentials  $E_{1/2}$  values, as anticipated, successively become more positive with the increasing number of fluorine atoms (Table IX).

(24) Jubran, N.; Meyerstein, D.; Koresh, J.; Cohen, H. *J. Chem. Soc., Dalton Trans.* **1986**, 2509. It is worthy of note that the redox potential of the Ni(III/II) couple is lowered in Na<sub>2</sub>SO<sub>4</sub> as compared to NaClO<sub>4</sub> because of the coordination of SO<sub>4</sub><sup>2-</sup> to Ni(III).

(22) (a) Thöm, V. J.; Boeyens, J. C. A.; McDougall, G. J.; Hancock, R. D. *J. Am. Chem. Soc.* **1984**, *106*, 3198. (b) Barefield, E. K.; Bianchi, A.; Billo, E. J.; Connolly, P. J.; Paoletti, P.; Summers, J. S.; Van Derveer, D. G. *Inorg. Chem.* **1986**, *25*, 4197.

(23) (a) Bosnich, B.; Mason, R.; Pauling, P. J.; Robertson, G. B.; Tobe, M. L. *Chem. Commun.* **1965**, 97. (b) Ito, T.; Kato, M.; Ito, H. *Bull. Chem. Soc. Jpn.* **1984**, *57*, 2641.

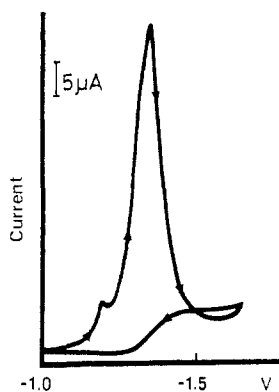
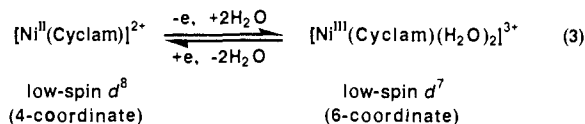
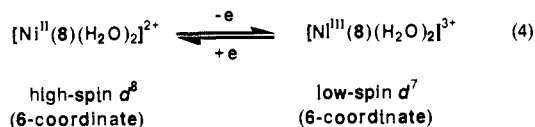


**Figure 6.** Current-potential curve for the tetrafluorinated cyclam-Ni(II) complex **25**·(ClO<sub>4</sub>)<sub>2</sub> (1.0 mM) in 0.1 M NaClO<sub>4</sub> aqueous solution (pH 4.0) under CO<sub>2</sub>. Using hanging mercury electrode, V vs Ag/AgCl; scan rate, 100 mV/s.

The reaction entropies associated with the Ni(III/II) redox change were estimated from the slope of the straight lines for  $E_{1/2}$  vs temperature ( $T$ ) plots,<sup>25</sup> as for the nonfluorinated cyclam complex **22**, where  $\Delta S^\circ_{rc}$  was +34.3 cal mol<sup>-1</sup> K<sup>-1</sup> starting from the 100% low-spin Ni(II) complex (attained in 3.5 M NaClO<sub>4</sub> solution).<sup>26</sup> This fact was interpreted to represent a reaction (3)



involving stronger hydrations in going to Ni(III).<sup>27</sup> On the other hand, with the present [Ni<sup>II</sup>-**8**](ClO<sub>4</sub>)<sub>2</sub> complex (>99% high-spin state in 0.1 M NaClO<sub>4</sub> aqueous solution at <30 °C), the  $E_{1/2}$  values between 10 and 30 °C gave the  $\Delta S^\circ_{rc}$  value of +10.4 cal mol<sup>-1</sup> K<sup>-1</sup> (Figure 5). This smaller  $\Delta S^\circ_{rc}$  value may be ascribed to a lesser change in the complex-water interaction and may reflect difficulty (due to the lipophilic nature of **8**) in more solvation to be demanded for the Ni<sup>II</sup> → Ni<sup>III</sup> process (see eq 4).



The reduction potentials for Ni(II/I) in aqueous solution<sup>28</sup> were also determined in Ar atmosphere by the reversible cyclic voltammograms (for **8**, see Figure 4b), and the results are summarized in Table IX. As the number of fluorines increases,  $E_{1/2}$  become successively less negative values, indicating the Ni(I) complexes become more stabilized. Here again, the electron-withdrawing effect and lipophilic effect of F should work to favor the complexes in the lower oxidation state.

**A Preliminary Test of the Ni(II) Complexes of Fluorinated Cyclams for Electrocatalytic Reduction of CO<sub>2</sub> in H<sub>2</sub>O.** Recently, a Ni(II)-cyclam complex was found to become an extremely selective electrocatalyst through Ni(I) for CO<sub>2</sub> reduction to CO in water.<sup>1b,29</sup> The present fluorinated cyclams, which favor Ni(I)

**Table X.** Efficiency and Selectivity in Electrochemical Reduction of CO<sub>2</sub> to CO<sup>a</sup>

electrocatalyst	appl potenti (V vs SCE)	generated CO, mL	turnover freq on Ni(II) complex, h <sup>-1</sup>	H <sub>2</sub> /CO in gas prodcd
[Ni <sup>II</sup> - <b>5</b> ](Cl <sub>2</sub> ) ( <b>22</b> ·Cl <sub>2</sub> )	-1.30	14.7	44	2.1 × 10 <sup>-4</sup>
[Ni <sup>II</sup> - <b>6</b> ](ClO <sub>4</sub> ) <sub>2</sub> [ <b>23</b> ·(ClO <sub>4</sub> ) <sub>2</sub> ]	-1.30	10.2	31	1.5 × 10 <sup>-3</sup>
[Ni <sup>II</sup> - <b>7</b> ](Cl <sub>2</sub> ) ( <b>24</b> ·Cl <sub>2</sub> )	-1.30	4.1	12	3.4 × 10 <sup>-3</sup>
[Ni <sup>II</sup> - <b>8</b> ](Cl <sub>2</sub> ) ( <b>25</b> ·Cl <sub>2</sub> )	-1.30	2.9	9	0.20
[Ni <sup>II</sup> - <b>8</b> ](ClO <sub>4</sub> ) <sub>2</sub> [ <b>25</b> ·(ClO <sub>4</sub> ) <sub>2</sub> ]	-1.30	1.4	4	0.22
[Ni <sup>II</sup> - <b>5</b> ](Cl <sub>2</sub> ) ( <b>22</b> ·Cl <sub>2</sub> )	-1.10	0.02	0.06	0.14
[Ni <sup>II</sup> - <b>8</b> ](ClO <sub>4</sub> ) <sub>2</sub> [ <b>25</b> ·(ClO <sub>4</sub> ) <sub>2</sub> ]	-1.10	0.82	2.5	6.6 × 10 <sup>-3</sup>

<sup>a</sup> For experimental conditions, see Experimental Section; [Ni<sup>II</sup>L] (where L = **5-8**) = 1.7 × 10<sup>-4</sup> M in 0.1 M KNO<sub>3</sub> (pH 4.1). Electrolysis time, 4 h. Temperature, 25 ± 3 °C.

complexes, were anticipated to find a useful application in this reaction.

The reversible Ni(II/I) couples observed in Ar atmosphere for all the F-cyclam complexes became irreversible in CO<sub>2</sub> atmosphere, a clear indication of the catalytic reduction of CO<sub>2</sub>. Typical current-potential curves for the tetrafluorinated **25**·(ClO<sub>4</sub>)<sub>2</sub> under CO<sub>2</sub> are shown in Figure 6.

Table X compares the catalytic efficiencies in the controlled-potential (-1.30 V) electrolysis of CO<sub>2</sub>-saturated aqueous solution under common conditions. The nonfluorinated cyclam **5** was first tested at -1.30 V vs SCE at the Hg electrode as a good check with the literature data (turnover frequency, 32 h<sup>-1</sup>; H<sub>2</sub>/CO ratio, 3 × 10<sup>-4</sup>).<sup>1b</sup> The efficiency of (CO + H<sub>2</sub>) gas production and the selectivity of H<sub>2</sub>/CO markedly depended upon the number of fluorine atom(s). The CO yield decreased with increased ratio of H<sub>2</sub>, as the number of fluorines increased. We have spectroscopically confirmed that the fluorinated catalysts were stable in the CO<sub>2</sub> reduction course.

However, when the potential was -1.10 V, the tetrafluorinated cyclam-Ni(II) complex **25**·(ClO<sub>4</sub>)<sub>2</sub> showed more efficient and selective catalytic activity (turnover frequency, 2.5 h<sup>-1</sup>; H<sub>2</sub>/CO ratio, 6.6 × 10<sup>-3</sup>) than the nonfluorinated cyclam complex **22**·Cl<sub>2</sub> (0.06 and 0.14, respectively). More elaborate work on **25** might find it even surpassing the catalytic efficiency that was found for **22** at higher energy (-1.30 V).

## Conclusion

Synthesis of the mono-, di-, and tetrafluorinated dioxocyclams (**2-4**) and cyclams (**6-8**) has been accomplished. An electron-withdrawing effect and a lipophilic effect of fluorine atoms on ligand properties were demonstrated by the weakened amine basicities and LF strengths with successive fluorine substitutions with respect to those for nonfluorinated **1** and **5**. However, the fluorinated **2-4** exhibit higher formation constants of square-planar [Cu<sup>II</sup>(H<sub>2</sub>L)]<sup>0</sup> complexes. In their kinetics in acetate buffers (4.7 < pH < 5.7), the fastest overall complexation was observed with the tetrafluorinated **4**, where the contribution of the unprotonated ligand form is most determining. With Ni(II) complexes of cyclams **5-8** in aqueous solution, the ratio of the octahedral, high-spin state increases as the number of fluorine atoms increases. The tetrafluorinated complex **25** is in almost 100% high-spin state. The fluorine substitution strongly affects the electrochemical properties of Cu(II) and Ni(II) complexes. In both [Cu<sup>II</sup>(H<sub>2</sub>L)]<sup>0</sup> **19-21** and [Ni<sup>II</sup>L]<sup>2+</sup> **23-25**, the higher oxidation states Cu(III) and Ni(III) become successively destabilized with respect to Cu(II) and Ni(II), while the lower oxidation state Ni(I) becomes successively stabilized with respect to Ni(II). The X-ray crystal structure of the **8** complex with NiCl<sub>2</sub> showed an octahedral, high-spin form, where the bonding parameters are similar to those for the nonfluorinated cyclam **5** complex. A preliminary test,

(25) (a) Yee, E. L.; Cave, R. J.; Guyer, K. L.; Tyma, P. D.; Weaver, M. J. *J. Am. Chem. Soc.* **1979**, *101*, 1131. (b) Hupp, J.; Weaver, M. J. *Inorg. Chem.* **1984**, *23*, 3639, and references cited therein.

(26) Fabbri, L.; Paoletti, A.; Profumo, A.; Soldi, T. *Inorg. Chem.* **1986**, *25*, 4256.

(27) (a) LoVecchio, F. V.; Gore, E. S.; Busch, D. H. *J. Am. Chem. Soc.* **1974**, *96*, 3109. (b) Sabatini, L.; Fabbri, L. *Inorg. Chem.* **1979**, *18*, 438.

(28) (a) Zeigerson, E.; Ginzburg, G.; Schwartz, N.; Luz, Z.; Meyerstein, D. *J. Chem. Soc., Chem. Commun.* **1979**, 241. (b) Jubran, N.; Ginzburg, G.; Cohen, H.; Meyerstein, D. *J. Chem. Soc., Chem. Commun.* **1982**, 517. (c) Jubran, N.; Ginzburg, G.; Cohen, H.; Koresh, Y.; Meyerstein, D. *Inorg. Chem.* **1985**, *24*, 251.

(29) For recent reviews: (a) Collin, J. P.; Sauvage, J. P. *Coord. Chem. Rev.* **1989**, *93*, 245. (b) Taniguchi, I. *Modern Aspects of Electrochemistry*; Bockris, J. O'M., White, R. E.; Conway, B. E., Eds.; Plenum Publishing Co.: New York, 1989.



where Ni(II) complexes of the fluorinated cyclams were used as electrocatalysts for CO<sub>2</sub> reduction to CO in H<sub>2</sub>O, suggests a promising application of fluorinated cyclams in redox-involving cyclam chemistry.<sup>28b,c,30</sup>

(30) (a) Jubran, N.; Cohen, H.; Koresh, Y.; Meyerstein, D. *J. Chem. Soc., Chem. Commun.* **1984**, 1683. (b) Blake, A. J.; Gould, R. O.; Hyde, T. I.; Schröder, M. *J. Chem. Soc., Chem. Commun.* **1987**, 431.

**Acknowledgment.** The present study was supported by a Grant-in-Aid for Scientific Research, 01771933 (to M.S.), from the Ministry of Education, Science and Culture.

**Supplementary Material Available:** Listing of anisotropic thermal parameters (1 page); table of calculated and observed structure factors (5 pages). Ordering information is given on any current masthead page.

## Synthesis, X-ray Structure, and Spectroscopic and Electrochemical Properties of Novel Heteronuclear Ruthenium–Osmium Complexes with an Asymmetric Triazolate Bridge

Ronald Hage,<sup>1a</sup> Jaap G. Haasnoot,<sup>\*1a</sup> Heleen A. Nieuwenhuis,<sup>1a</sup> Jan Reedijk,<sup>1a</sup> Dirk J. A. De Ridder,<sup>1b</sup> and Johannes G. Vos<sup>\*1c</sup>

Contribution from the Department of Chemistry, Gorlaeus Laboratories, Leiden University, P.O. Box 9502, 2300 RA Leiden, The Netherlands, Laboratory of Crystallography, University of Amsterdam, Nieuwe Achtergracht 166, 1018 WV Amsterdam, The Netherlands, and School of Chemical Sciences, Dublin City University, Dublin 9, Ireland. Received May 9, 1990

**Abstract:** The heterodinuclear compounds [(bpy)<sub>2</sub>Ru(bpt)Os(bpy)<sub>2</sub>](PF<sub>6</sub>)<sub>3</sub> (RuOs) and [(bpy)<sub>2</sub>Os(bpt)Ru(bpy)<sub>2</sub>](PF<sub>6</sub>)<sub>3</sub> (OsRu), where Hbpt = 3,5-bis(pyridin-2-yl)-1,2,4-triazole and bpy = 2,2'-bipyridine, have been prepared and characterized. The crystal and molecular structures of [(Ru(bpy)<sub>2</sub>)<sub>2</sub>(bpt)](CF<sub>3</sub>SO<sub>3</sub>)<sub>3</sub>·4H<sub>2</sub>O and [(bpy)<sub>2</sub>Ru(bpt)Os(bpy)<sub>2</sub>](CF<sub>3</sub>SO<sub>3</sub>)<sub>3</sub>·4H<sub>2</sub>O have been determined. The dinuclear ruthenium(II) compound crystallizes in the monoclinic space group *P*2<sub>1</sub>/*c* with four molecules in a cell of dimensions *a* = 13.510 (1) Å, *b* = 16.110 (2) Å, *c* = 29.861 (4) Å, β = 99.225 (9)°. Only one of the two possible geometrical isomers of the ruthenium dinuclear compound was found in the crystal structure. The two metal centers are coordinated via N(1) and N(4) of the triazole ring with a Ru(1)–N(1) distance of 2.03 (1) Å and a Ru(2)–N(4) distance of 2.11 (1) Å. The metal–metal distance is 6.184 (2) Å. In [(bpy)<sub>2</sub>Ru(bpt)Os(bpy)<sub>2</sub>](CF<sub>3</sub>SO<sub>3</sub>)<sub>3</sub>·4H<sub>2</sub>O with *Z* = 4, *P*2<sub>1</sub>/*c*, *a* = 13.5802 (7) Å, *b* = 16.247 (2) Å, *c* = 30.043 (3) Å, β = 100.348 (6)°, ruthenium is coordinated via N(1), whereas osmium binds via N(4) of triazole with similar metal–nitrogen distances as observed for the ruthenium homonuclear compounds. The NMR data revealed that the OsRu isomer has a similar structure, but with the osmium center bound via N(1) and the ruthenium ion coordinated via N(4) of the triazole ring. The electrochemical potentials of the two heterodinuclear compounds are significantly different: for the RuOs compound the oxidation potentials are 0.73 and 1.20 V, while for the OsRu isomer the oxidation potentials are at 0.65 and 1.30 V vs SCE. These differences in electrochemical behavior between the two isomeric RuOs and OsRu compounds suggest that the N(1) atom of the triazole ring is a better σ-donor than N(4). The mixed-valence dinuclear systems all exhibit rather intense intervalence transition (IT) bands in the near-infrared region, suggesting a moderately strong metal–metal interaction for the bpt systems. A correlation between the energy of the IT bands of the mixed-valence dinuclear complexes and the oxidation potentials has been observed.

### Introduction

[Ru(bpy)<sub>3</sub>]<sup>2+</sup> (bpy = 2,2'-bipyridine) and related complexes have been the subject of many investigations because of their varied photophysical and electrochemical properties.<sup>1–6</sup> Also dinuclear ruthenium and osmium compounds have been the subject of much research, not only because of their possible application as two-

electron-transfer reagents in water splitting devices, but also because of the current interest in the properties of mixed-valence compounds,<sup>7–12</sup> the theory of which has been developed in detail by Hush.<sup>13</sup>

(1) (a) Leiden University. (b) University of Amsterdam. (c) Dublin City University.

(2) Seddon, E. A.; Seddon, K. R. *The Chemistry of Ruthenium*; Elsevier Science Publisher BV: Amsterdam, 1984.

(3) (a) Meyer, T. J. *Acc. Chem. Res.* **1978**, *11*, 94. (b) Meyer, T. J. *Pure Appl. Chem.* **1986**, *58* (9), 1193.

(4) Juris, A.; Balzani, V.; Barigelletti, F.; Belser, P.; von Zelewsky, A. *Coord. Chem. Res.* **1988**, *84*, 85.

(5) Kalyanasundaram, K.; Grätzel, M.; Pelizzetti, E. *Coord. Chem. Rev.* **1986**, *69*, 57.

(6) Krause, R. A. *Struct. Bonding* **1987**, *67*, 1.

(7) (a) Haga, M.; Matsumura-Inoue, T.; Yanabe, S. *Inorg. Chem.* **1987**, *26*, 4148. (b) Neyhart, G. A.; Meyer, T. J. *Inorg. Chem.* **1986**, *25*, 4807. (c) Hupp, J. T.; Neyhart, G. A.; Meyer, T. J. *J. Am. Chem. Soc.* **1986**, *108*, 5349. (d) Furue, M.; Kinashita, S.; Kushida, T. *Chem. Lett.* **1987**, 2355. (e) Kalyanasundaram, K.; Nazceeruddin, Md. K. *Chem. Phys. Lett.* **1989**, *158*, 45.

(8) Sahai, R.; Baucom, D. A.; Rillema, D. P. *Inorg. Chem.* **1986**, *25*, 3843. (9) (a) Kober, E. M.; Goldsby, K. A.; Narayana, D. N. S.; Meyer, T. J. *J. Am. Chem. Soc.* **1983**, *105*, 4303. (b) Schanze, K. S.; Neyhart, G. A.; Meyer, T. J. *J. Phys. Chem.* **1986**, *90*, 2182.

(10) Goldsby, K. A.; Meyer, T. J. *Inorg. Chem.* **1984**, *23*, 3002.

(11) (a) Kober, E. M. Thesis, North Carolina, 1982. (b) Kober, E. M.; Meyer, T. J. *Inorg. Chem.* **1984**, *23*, 3877. (c) Kober, E. M.; Meyer, T. J. *Inorg. Chem.* **1982**, *21*, 3967.

(12) (a) Curtis, J. C.; Bernstein, J. S.; Meyer, T. J. *Inorg. Chem.* **1985**, *24*, 385. (b) Schanze, K. S.; Meyer, T. J. *Inorg. Chem.* **1985**, *24*, 2122.